Torsional vibrations of circular elastic plates with thickness steps

M.K. Kang, Rui Huang[a)]

Research Center for Mechanics of Solids, Structures & Materials

Department of Aerospace Engineering and Engineering Mechanics

The University of Texas, Austin, Texas 78712

T. Knowles

Texzec, Inc., Round Rock, Texas 78681

Submitted on July 25, 2004

(Running title): Circular plates with thickness steps

[a)] Corresponding author. Electronic mail: ruihuang@mail.utexas.edu.

Abstract

This paper presents a theoretical study of torsional vibrations in isotropic elastic plates. First, the exact solutions for torsional vibrations in circular and annular plates are reviewed. Then, an approximate method is developed to analyze torsional vibrations of circular plates with thickness steps. The method is based on an approximate plate theory for torsional vibrations derived from the variational principle following Mindlin's series expansion method. Approximate solutions for the zeroth- and first-order torsional modes in the circular plate with one thickness step are presented. It is found that, within a narrow frequency range, the first-order torsional modes can be trapped in the inner region when the thickness exceeds that of the outer region. The mode shapes clearly show that both the displacement and the stress amplitudes decay exponentially away from the thickness step. The existence and the number of the trapped first-order torsional modes in a circular mesa on an infinite plate are determined as functions of the normalized geometric parameters, which may serve as a guide for designing distributed torsional-mode resonators for sensing applications.

ASA-PACS numbers: 43.40.Dx, 43.40.At, 43.20.Bi, 43.20.Ks

I. INTRODUCTION

Torsional vibrations of circular plates and cylindrical rods have been studied for many years. Recent developments of torsional-mode sensors and actuators in micro- and nano-electromechanical systems have renewed interests in this topic[1-5]. Previous studies of torsional vibrations have largely focused on cylindrical rods or shafts, for which a one-dimensional mathematical model based on the "strength-of-materials" approach[6] has been widely used in practice. However, it has been shown that the one-dimensional model is only accurate at low frequencies and three-dimensional analysis is required at high frequencies[7]. In particular, shafts with stepped cross-sections are common in engineering structures. Several three-dimensional methods have been developed to analyze torsional vibrations of stepped shafts[7-11]. Johnson et al.[11] showed that, within a certain frequency range, torsional modes can be trapped in the central section of stepped solid cylinders with a slightly larger diameter such that the vibration amplitude decays exponentially with the distance from the central section. Such trapped modes may find interesting applications in the design of resonators, transducers, and sensors.

Vibrational energy trapping in plates has been a subject of considerable interest because of its importance in the design of quartz crystal oscillators. By electroplating of quartz crystal plates, thickness-shear vibrations can be trapped near the electrodes with amplitude decreasing exponentially away from the electrodes in the unplated region[12-16]. It has also been observed that, by decreasing the plate thickness from center to edge or contouring, the thickness-shear vibrations can be confined in the center portion of the plate, which improves the resonator performance by reducing edge leakage due to boundary mismatch and mode conversion[17-19]. Much less attention has been paid to torsional vibrations of plates. By using Love's thin plate theory[20], Onoe[21] analyzed the contour vibrations of circular plates including torsional modes

(Onoe used the term “tangential modes”). The result was used by Meitzler[22] in an ultrasonic technique for determining elastic constants of glass wafers. For thick plates, exact solutions are available for both solid circular plates and annular plates, which are essentially the same as the exact solutions to the classical Pochhammer equation for cylindrical rods and hollow cylinders[23,24]. For plates with non-uniform thickness, an exact analytical solution is generally not possible[25]. This paper develops an approximate method for analyzing torsional vibrations of circular plates with thickness varying in the radial direction as steps (e.g., Figure 1c). Such plates are of interest because torsional vibrations may be trapped near the steps, similar to that in stepped solid cylinders[11] and the thickness-shear vibrations in contoured plates[17-19]. Recent experiments by Knowles et al.[26] have observed trapped torsional modes in stepped and contoured aluminum plates, which may be used to design sensors with improved performance in the presence of liquids.

The paper is organized as follows. Section 2 reviews the general three-dimensional theory and exact solutions for torsional vibrations of circular and annular plates with uniform thickness (Figure 1a&b). Section 3 develops an approximate plate theory from variational principle. In Section 4, an approximate method is developed for torsional vibrations of plates with thickness steps (Figure 1c), and approximate solutions are obtained for the zeroth- and first-order modes. Trapped first-order modes are identified. A map is constructed predicting the existence and the number of the trapped torsional modes in a circular mesa on an infinite plate. Section 5 concludes with remarks on potential applications of the theoretical results.

II. GENERAL THEORY AND EXACT SOLUTIONS

Figure 1 illustrates the geometries of the plates considered in this paper. Assuming axisymmetric motion and isotropic, linear elastic materials, the momentum equation for the torsional motion is

$$\frac{\partial^2 u_\theta}{\partial r^2}+\frac{1}{r}\frac{\partial u_\theta}{\partial r}-\frac{u_\theta}{r^2}+\frac{\partial^2 u_\theta}{\partial z^2}=\frac{\rho}{\mu}\frac{\partial^2 u_\theta}{\partial t^2}, \tag{1}$$

where r, θ, z are the cylindrical coordinates as defined in Figure 1, t is the time, u_θ is the torsional displacement, ρ is the mass density, and μ is the shear modulus.

The stress associated with the torsional motion has two nonzero shear components, which relate to the torsional displacement by

$$\sigma_{z\theta}=\mu\frac{\partial u_\theta}{\partial z}, \tag{2}$$

$$\sigma_{r\theta}=\mu\left(\frac{\partial u_\theta}{\partial r}-\frac{u_\theta}{r}\right). \tag{3}$$

For plates with uniform thickness, Eq. (1) can be solved by separation of variables. Assume a harmonic solution, namely

$$u_\theta(r,z,t)=P(r)Q(z)e^{i\omega t}, \tag{4}$$

where ω is the angular frequency of vibration. Substitution of Eq. (4) into Eq. (1) leads to

$$\frac{d^2P}{dr^2}+\frac{1}{r}\frac{dP}{dr}+\left(\beta^2-\frac{1}{r^2}\right)P=0, \tag{5}$$

$$\frac{d^2Q}{dz^2}+k^2Q=0, \tag{6}$$

where

$$\beta^2+k^2=\frac{\rho\omega^2}{\mu}. \tag{7}$$

For $\beta, k \neq 0$, the general solutions to Eqs. (5) and (6) are,

$$P(r) = AJ_1(\beta r) + BY_1(\beta r)\,, \tag{8}$$

$$Q(z) = C\sin(kz) + D\cos(kz)\,, \tag{9}$$

where J_1 and Y_1 are the first-order Bessel functions of the first and second kinds, respectively, and the coefficients A, B, C, D must be determined from boundary conditions. An alternative form of the solution (8) is

$$P(r) = AH_1^{(1)}(\beta r) + BH_1^{(2)}(\beta r)\,, \tag{10}$$

where $H_1^{(1)}$ and $H_1^{(2)}$ are the first-order Hankel functions of the first and second kinds. Due to their asymptotic behavior, the Hankel functions sometimes offer convenience for physical interpretations of the solution.

When $\beta = 0$, the solution (8) is replaced by a special solution

$$P(r) = Ar + \frac{B}{r}\,. \tag{11}$$

Similarly, when $k = 0$, the solution (9) is replaced by

$$Q(z) = Cz + D\,. \tag{12}$$

A complete solution for free vibrations can be obtained by a superposition of all possible solutions in the form of Eq. (4) with the value of β or k determined from the boundary condition. For forced vibrations, a particular solution satisfying the forcing boundary conditions must be included in the superposition. This paper focuses on free vibrations only.

A. Free vibrations of a circular plate

First consider a circular plate of radius a and thickness h with traction-free boundaries at all surfaces and edges (Figure 1a). The boundary condition requires that

$$\frac{dP}{dr} - \frac{P}{r} = 0 \qquad \text{at r} = a. \tag{13}$$

$$\frac{dQ}{dz} = 0 \qquad \text{at } z = 0 \text{ and } h. \tag{14}$$

In addition, it is implied that the displacement at the center of the plate (r = 0) is finite. Consequently, any singular terms with respect to r must be discarded from the solution. Therefore,

$$P_m(r) = \begin{cases} A_0 r & m = 0 \\ A_m J_1(\beta_m r) & m = 1,2,\cdots \end{cases}, \tag{15}$$

where $\beta_m = s_m / a$ and s_m is the mth nonzero root to $J_2(s) = 0$, and

$$Q_n(z) = D_n \cos(k_n z), \tag{16}$$

where $k_n = \dfrac{n\pi}{h}$ for n = 0, 1, 2, ….

Combining Eqs. (15) and (16), one obtains the complete solution for torsional vibrations of the circular plate, namely

$$\begin{aligned} u_\theta(r,z,t) = \sum_{n=0}^{\infty} \Big[& A_n r \cos(k_n z) e^{i\omega_n t} \\ & + \sum_{m=1}^{\infty} B_{mn} J_1(\beta_m r) \cos(k_n z) e^{i\omega_{mn} t} \Big], \end{aligned} \tag{17}$$

where

$$\omega_n = \frac{n\pi}{h}\sqrt{\frac{\mu}{\rho}}, \tag{18}$$

$$\omega_{mn} = \sqrt{\frac{\mu}{\rho}\left(\frac{n^2\pi^2}{h^2} + \frac{s_m^2}{a^2}\right)}. \tag{19}$$

Solution (17) consists of all the possible torsional modes that satisfy the boundary conditions for the circular plate, where Eqs. (18) and (19) give the corresponding resonant frequency of each mode.

Figure 2 shows the spectrum for torsional vibrations of circular plates, where the frequency is normalized by the first cut-off frequency, $\omega_1 = \frac{\pi}{h}\sqrt{\frac{\mu}{\rho}}$, and plotted against the ratio between the thickness and the radius of the plate. The spectrum includes two limiting cases. To the right end of the spectrum, *h*/*a* >> 1, and the first several modes with the lowest frequencies correspond to the case with $\beta = 0$. In this case, the displacement is proportional to the *r*-coordinate as given by the first term in the bracket of Eq. (17), and the resonance frequencies (ω_n) are independent of the radius of the plate. These modes are identical to those predicted by the one-dimensional model for long cylindrical rods. To the left end of the spectrum, *h*/*a* << 1, and the first several modes with the lowest frequencies now correspond to the case with *k* = 0 (*n* = 0), for which the displacement is independent of z and the resonance frequency independent of the thickness *h*. These modes are identical to those predicted by Onoe[21] for thin circular plates. Between the two limits, the frequencies from different groups are interwoven. The spectrum clearly shows when the one-dimensional model or the thin-plate approximations can be used and when the exact three-dimensional analysis is required. Zhou et al.[27] recently conducted a three-dimensional vibration analysis using the Chebyshev-Ritz method and predicted the first 10 resonance frequencies for a circular plate with thickness ratio *h*/*a* = 0.4, as shown by the circles in Figure 2. The excellent agreement confirms the accuracy of the Chebyshev-Ritz method.

B. Free vibrations of annular plates

Next consider an annular plate with outer radius *a*, inner radius *b*, and thickness *h* (Figure 1b). Both inner and outer edges are traction free. In addition to the boundary conditions (13) and (14), the traction-free condition at the inner edge requires that

$$\frac{dP}{dr} - \frac{P}{r} = 0 \quad \text{at r} = b. \tag{20}$$

Consequently, Eq. (15) becomes

$$P_m(r) = \begin{cases} A_0 r & m = 0 \\ A_m\left[Y_2(\beta_m a)J_1(\beta_m r) - J_2(\beta_m a)Y_1(\beta_m r)\right] & m = 1,2,\cdots \end{cases}, \tag{21}$$

where $\beta_m = s_m / a$ and here s_m is the *m*th root to the following equation,

$$J_2(s)Y_2(\eta s) - J_2(\eta s)Y_2(s) = 0\,, \tag{22}$$

with $\eta = b/a$. Equation (21) recovers Eq. (15) when the inner radius *b* = 0.

With Eq. (16) unchanged, the complete solution for torsional vibrations of the annular plate is

$$\begin{aligned} u_\theta(r,z,t) = \sum_{n=0}^{\infty}\Big[&A_n r\cos(k_n z)e^{i\omega_n t} \\ &+ \sum_{m=1}^{\infty} B_{mn}\big(Y_2(\beta_m a)J_1(\beta_m r) - J_2(\beta_m a)Y_1(\beta_m r)\big)\cos(k_n z)e^{i\omega_{mn} t}\Big] \end{aligned}, \tag{23}$$

where the frequencies ω_n and ω_{mn} take the same form as in Eqs. (18) and (19).

The frequency spectrum for the annular plates is similar to Figure 2, but the radial wave number β_m varies with η, the ratio between the inner radius and the outer radius. Figure 3 shows the first five radial wave numbers obtained from Eq. (22) as functions of the ratio. The left end of the figure corresponds to the case of solid circular plates ($\eta = 0$). Toward the right end, the wave numbers rise rapidly, which correspond to thin-wall tubes. Similar result was obtained by Clark[23] for hollow cylinders.

Following similar procedures, exact solutions for torsional vibrations of circular and annular plates with other boundary conditions can be obtained. For plates with non-uniform thickness, however, exact solutions are generally not available[25]. Consider a circular plate with a thickness step (Figure 1c), which has thickness h_1 at the inner region ($0 < r < b$) and thickness h_2 ($h_2 \neq h_1$) at the outer region ($b < r < a$). The general solution for torsional vibrations of such plates should consist of two parts: For the inner region, the displacement takes the form of Eq. (17); for the outer region, the displacement takes the form of Eq. (23). The two parts are coupled through the joint boundary at $r = b$, where the continuity conditions for the displacement and the shear traction have to be applied. However, exact solutions satisfying the continuity conditions cannot be obtained analytically. The remainder of this paper develops an approximate plate theory, from which approximate solutions to torsional vibrations of circular plates with thickness steps are obtained.

III. APPROXIMATE PLATE THEORY

A general procedure for deducing approximate equations for elastic plates from the three-dimensional theory of elasticity was first introduced by Mindlin[28] based on the series expansion methods of Poisson[29] and Cauchy[30] and the variational method of Kirchhoff[31]. The procedure has been used to derive approximate plate theories for both elastic and piezoelectric crystal plates with uniform[32-34] and nonuniform thickness[35, 18, 19]. Here we follow the same procedure to derive approximate equations for torsional vibrations of isotropic elastic plates. The approximate equations will then be used to deduce an approximate solution to torsional vibrations of circular plates with thickness steps in the next section.

Considering torsional motion of a linear elastic continuum of volume V bounded by a surface S, the variational principle leads to

$$\int dt \int_V \left(\frac{\partial \sigma_{r\theta}}{\partial r} + \frac{\partial \sigma_{z\theta}}{\partial z} + \frac{2\sigma_{r\theta}}{r} - \rho \frac{\partial^2 u_\theta}{\partial t^2} \right) \delta u_\theta dV = 0 , \tag{24}$$

$$\int dt \int_S \left(t_\theta - n_r \sigma_{r\theta} - n_z \sigma_{z\theta} \right) \delta u_\theta dS = 0 , \tag{25}$$

where t_θ is the traction at boundary S, and **n** is the outward normal at the boundary. For a circular plate (Figure 1a), the boundary S consists of two surfaces at z = 0 and h and the edge face at r = a. For an annular plate (Figure 1b), another edge at r = b adds to the boundary.

Expand the displacement into a cosine series,

$$u_\theta(r,z,t) = \sum_{n=0}^{\infty} u_\theta^{(n)}(r,t) \cos\left(n\pi \frac{z}{h} \right) . \tag{26}$$

The orthogonality of the cosine series leads to

$$u_\theta^{(n)}(r,t) = \frac{2-\delta_{n0}}{h} \int_0^h u_\theta(r,z,t) \cos\left(n\pi \frac{z}{h} \right) dz , \tag{27}$$

where $\delta_{mn} = 1$ if $m = n$ and $\delta_{mn} = 0$ otherwise.

Substituting Eq. (26) into Eq. (24) and integrating over the thickness of the plate, we obtain that

$$\begin{gathered} \int dt \int_A \sum_{n=0}^{\infty} \left[\sigma_{r\theta,r}^{(n)} + \frac{2}{r} \sigma_{r\theta}^{(n)} + \frac{n\pi}{h} \bar{\sigma}_{z\theta}^{(n)} \right. \\ \left. + \frac{1}{h} F_\theta^{(n)} - \frac{1+\delta_{n0}}{2} \rho \ddot{u}_\theta^{(n)} \right] \delta u_\theta^{(n)} dA = 0 \end{gathered} , \tag{28}$$

where A is a plane parallel to the surface of the plate, and

$$\sigma_{r\theta}^{(n)} = \frac{1}{h}\int_0^h \sigma_{r\theta} \cos\left(n\pi \frac{z}{h} \right) dz \,, \tag{29}$$

$$\bar{\sigma}_{z\theta}^{(n)} = \frac{1}{h}\int_0^h \sigma_{z\theta} \sin\left(n\pi \frac{z}{h} \right) dz \,, \tag{30}$$

$$F_\theta^{(n)} = (-1)^n \sigma_{z\theta}(h) - \sigma_{z\theta}(0) \,. \tag{31}$$

In a similar manner, substituting Eq. (26) into Eq. (25), we obtain that

$$\int dt \int_C \sum_{n=0}^{\infty} \left[t_\theta^{(n)} - n_r \sigma_{r\theta}^{(n)} \right] \delta u_\theta^{(n)} ds = 0 \,, \tag{32}$$

where C is the contour of the plate edge(s), and

$$t_\theta^{(n)} = \frac{1}{h}\int_0^h t_\theta \cos\left(n\pi \frac{z}{h} \right) dz \,. \tag{33}$$

In deriving Eq. (32), the integral over the two surfaces of the plate has been set zero as the surface traction is specified through the definition of $F_\theta^{(n)}$ in Eq. (31).

For Eqs. (28) and (32) to be true for arbitrary variations, we have, in A,

$$\sigma_{r\theta,r}^{(n)} + \frac{2}{r}\sigma_{r\theta}^{(n)} + \frac{n\pi}{h}\bar{\sigma}_{z\theta}^{(n)} + \frac{1}{h}F_\theta^{(n)} = \frac{1+\delta_{n0}}{2}\rho \ddot{u}_\theta^{(n)} \,, \tag{34}$$

and the boundary condition on C,

$$t_\theta^{(n)} = n_r \sigma_{r\theta}^{(n)} \text{ or } u_\theta^{(n)} = \hat{u}_\theta^{(n)} \,, \tag{35}$$

where $\hat{u}_\theta^{(n)}$ is any specified displacement at the edge. As a result, the three-dimensional problem described by Eqs. (24) and (25) has been transformed to a system of two-dimensional equations.

By inserting Eq. (26) into Eqs. (2) and (3) and then into Eqs. (29) and (30), we obtain that

$$\sigma_{r\theta}^{(n)} = \mu \frac{1+\delta_{n0}}{2} \left[\frac{\partial u_\theta^{(n)}}{\partial r} - \frac{u_\theta^{(n)}}{r} \right], \tag{36}$$

$$\bar{\sigma}_{z\theta}^{(n)} = -\mu \frac{n\pi}{2} \frac{u_\theta^{(n)}}{h} \,. \tag{37}$$

Substitution of Eqs. (36) and (37) into Eq. (34) leads to

$$\mu\left[\frac{\partial^2 u_\theta^{(n)}}{\partial r^2}+\frac{1}{r}\frac{\partial u_\theta^{(n)}}{\partial r}-\frac{u_\theta^{(n)}}{r^2}\right]-\mu\left(\frac{n\pi}{h}\right)^2 u_\theta^{(n)}+\frac{2-\delta_{n0}}{h}F_\theta^{(n)}=\rho\ddot{u}_\theta^{(n)}, \tag{38}$$

which is the *n*th-order displacement equation of torsional motion.

Each specific term in the infinite series expansion of the displacement in Eq. (26) can be obtained by solving Eq. (38) with associated boundary conditions at the edge(s) given by Eq. (35). For circular plates and annular plates with traction-free surfaces ($F_\theta^{(n)}=0$), the infinite series expansion is identical to the exact solutions in Eqs. (17) and (23). For circular plates with thickness steps (Figure 1c), specific displacement terms for the inner and outer regions can be obtained from Eq. (38) separately and the continuity condition at the step can be approximated by Eq. (35). The procedure is presented in the next section.

IV. APPROXIMATE SOLUTION FOR STEPPED PLATES

Figure 1c sketches the geometry of the plate under consideration. We assume an *n*th-order torsional motion in the inner region ($r < b$) but keep the series expansion of the displacement in the outer region ($b < r < a$) in order to satisfy the continuity conditions at the junction. Thus, the displacement of the stepped plate is

$$u_\theta(r,z,t)=\begin{cases} u_{\theta 1}^{(n)}(r,t)\cos\left(n\pi\dfrac{z}{h_1}\right), & r<b \text{ and } 0<z<h_1; \\ \displaystyle\sum_{m=0}^{\infty}u_{\theta 2}^{(m)}(r,t)\cos\left(m\pi\frac{z}{h_2}\right), & b<r<a \text{ and } 0<z<h_2. \end{cases} \tag{39}$$

Solving Eq. (38) for the inner and outer regions separately, we obtain that

$$u_{\theta 1}^{(n)}=A_1^{(n)}J_1(\beta_1^{(n)}r)e^{i\omega t}, \tag{40}$$

$$u_{\theta 2}^{(m)}=\left[A_2^{(m)}J_1(\beta_2^{(m)}r)+B_2^{(m)}Y_1(\beta_2^{(m)}r)\right]e^{i\omega t}, \tag{41}$$

where

$$\beta_1^{(n)2} = \frac{\rho}{\mu}\omega^2 - \left(\frac{n\pi}{h_1}\right)^2, \tag{42}$$

$$\beta_2^{(m)2} = \frac{\rho}{\mu}\omega^2 - \left(\frac{m\pi}{h_2}\right)^2. \tag{43}$$

The corresponding in-plane shear stresses are

$$\sigma_{r\theta 1}^{(n)} = -\frac{1+\delta_{n0}}{2}\mu A_1^{(n)}\beta_1^{(n)} J_2(\beta_1^{(n)} r) e^{i\omega t}, \tag{44}$$

$$\sigma_{r\theta 2}^{(m)} = -\frac{1+\delta_{m0}}{2}\mu \beta_2^{(m)}\left[A_2^{(m)} J_2(\beta_2^{(m)} r) + B_2^{(m)} Y_2(\beta_2^{(m)} r)\right] e^{i\omega t}. \tag{45}$$

At the junction (r = b), both the displacement and the traction are required to be continuous. In case of $h_1 > h_2$, part of the edge of the inner region is traction free with unspecified displacement. Thus, the continuity of the displacement is only required for $0 < z < h_2$, which, by Eq. (27), leads to

$$u_{\theta 2}^{(m)} = \frac{2-\delta_{m0}}{h_2}\int_0^{h_2} u_{\theta 1}^{(n)} \cos\left(n\pi\frac{z}{h_1}\right)\cos\left(m\pi\frac{z}{h_2}\right)dz. \tag{46}$$

On the other hand, the traction at the edge of the inner region is fully specified by the traction-free part and the continuous part, which requires that

$$\sigma_{r\theta 1}^{(n)} = \frac{1}{h_1}\int_0^{h_2}\sum_{m=0}^{\infty}(2-\delta_{m0})\sigma_{r\theta 2}^{(m)} \cos\left(m\pi\frac{z}{h_2}\right)\cos\left(n\pi\frac{z}{h_1}\right)dz. \tag{47}$$

Equations (46) and (47) represent the approximate continuity conditions at the thickness step. Substitution of Eqs. (40), (41), (44), and (45) into Eqs. (46) and (47) leads to

$$J_1(\beta_2^{(m)} b) A_2^{(m)} + Y_1(\beta_2^{(m)} b) B_2^{(m)} = \Lambda_{mn} J_1(\beta_1^{(n)} b) A_1^{(n)}, \tag{48}$$

$$\begin{aligned}&\sum_{m=0}^{\infty}(1+\delta_{m0})\Lambda_{mn}\beta_2^{(m)}h_2\left[J_2(\beta_2^{(m)}b)A_2^{(m)}+Y_2(\beta_2^{(m)}b)B_2^{(m)}\right]\\&\quad=(1+\delta_{n0})\beta_1^{(n)}h_1J_2(\beta_1^{(n)}b)A_1^{(n)}\end{aligned}, \tag{49}$$

where

$$\Lambda_{mn}=\frac{2-\delta_{m0}}{h_2}\int_0^{h_2}\cos\left(m\pi\frac{z}{h_2}\right)\cos\left(n\pi\frac{z}{h_1}\right)dz\,. \tag{50}$$

In addition, a traction-free condition at the outer edge (r = a) requires that

$$J_2(\beta_2^{(m)}a)A_2^{(m)}+Y_2(\beta_2^{(m)}a)B_2^{(m)}=0\,. \tag{51}$$

Equations (48), (49), and (51) form a linear system of infinite degrees (m = 0, 1, 2, …). In practice, only a finite subset of the equations may be used to obtain approximate solutions. Let m take values from 0 to M. The linear system takes the form

$$\Theta\cdot\mathbf{v}=0\,, \tag{52}$$

where Θ is a square matrix of size $2M+1$ and **v** is a vector consisting all the coefficients, $A_1^{(n)}$, $A_2^{(m)}$, and $B_2^{(m)}$. For nontrivial solutions, the determinant of the matrix vanishes, namely,

$$\det[\Theta]=0\,, \tag{53}$$

which gives the frequency equation for free vibrations of the stepped plate. The standard procedures of linear analysis can then be used to calculate the resonance frequencies and the corresponding mode shapes.

Similarly, for $h_1 < h_2$, the continuity conditions (46) and (47) become

$$u_{\theta1}^{(n)}=\frac{2-\delta_{n0}}{h_1}\int_0^{h_1}\sum_{m=0}^{\infty}u_{\theta2}^{(m)}\cos\left(m\pi\frac{z}{h_2}\right)\cos\left(n\pi\frac{z}{h_1}\right)dz\,, \tag{54}$$

$$\sigma_{r\theta2}^{(m)}=\frac{2-\delta_{n0}}{h_2}\int_0^{h_1}\sigma_{r\theta1}^{(n)}\cos\left(n\pi\frac{z}{h_1}\right)\cos\left(m\pi\frac{z}{h_2}\right)dz\,. \tag{55}$$

And Eqs. (48) and (49) become

$$\sum_{m=0}^{\infty} \overline{\Lambda}_{mn} \left[J_1(\beta_2^{(m)} b) A_2^{(m)} + Y_1(\beta_2^{(m)} b) B_2^{(m)} \right] = J_1(\beta_1^{(n)} b) A_1^{(n)} , \tag{56}$$

$$\begin{aligned} &(1+\delta_{m0})\beta_2^{(m)} h_2 \left[J_2(\beta_2^{(m)} b) A_2^{(m)} + Y_2(\beta_2^{(m)} b) B_2^{(m)} \right] \\ &\quad = (1+\delta_{n0})\overline{\Lambda}_{mn} \beta_1^{(n)} h_1 J_2(\beta_1^{(n)} b) A_1^{(n)} \end{aligned} \tag{57}$$

where

$$\overline{\Lambda}_{mn} = \frac{2-\delta_{n0}}{h_1} \int_0^{h_1} \cos\left(m\pi \frac{z}{h_2} \right) \cos\left(n\pi \frac{z}{h_1} \right) dz . \tag{58}$$

In the above approximation procedure, we have neglected coupling between torsion and flexure as well as possible stress singularity at the corner of the step[10]. The effect of these local events is considered negligible for the analysis of the global behavior of torsional vibrations.

A. Zeroth-order modes (*n* = 0)

First consider zeroth-order torsional vibrations in the inner region of a stepped plate, for which $n = 0$ and the displacement is independent of the thickness coordinate. Such modes are also called radial modes in thin circular plates. The displacement in the outer region in general consists of an infinite series expansion as in Eq. (39) in order to satisfy the continuity conditions at the step. Our calculations show that, for the zeroth-order modes, the first term ($m = 0$) in the expansion dominates and the effect of additional terms is negligible. Figure 4 shows the first three resonance frequencies of the zeroth-order modes varying with the radius of the inner region. The frequencies are normalized by the cut-off frequency, $\omega_1 = \frac{\pi}{h_1}\sqrt{\frac{\mu}{\rho}}$. The thickness ratio is fixed as $\frac{h_1}{h_2} = 1.1$ and the outer radius is $\frac{a}{h_2} = 10$. At both ends of the plot with the radius ratio b/a being 0 or 1, the stepped plate reduces to uniform circular plates with thickness h_2 and

h_1, respectively. The zeroth-order resonance frequencies of a uniform circular plate are given by Eq. (19) with n = 0 and labeled in Figure 4 as open squares. It is interesting to note that, while the zeroth-order resonance frequencies of a uniform circular plate are independent of its thickness and thus identical at both ends of Figure 4, the frequencies oscillate slightly in between, with the number of oscillations depending on the mode number and the amplitude of oscillation depending on the thickness of the step. Such oscillation may be caused by the interactions between the torsional waves and the discontinuous boundary at the step.

To check the continuity conditions at the step, Figure 5 plots the mode shape corresponding to point A (b/a = 0.2) labeled in Figure 4. It is noted that the displacement is continuous across the step but the stress by itself is not continuous. The error is due to the approximation of the traction continuity condition specified by Eq. (47), which leads to continuity of the total traction for the zeroth-order modes, i.e., $\sigma_{r\theta 1}^{(0)} h_1 = \sigma_{r\theta 2}^{(0)} h_2$ at $r = b$. Such approximation is reasonable for the zeroth-order modes when the thickness difference is small.

B. First-order modes (*n*=1)

Next consider the first-order modes with $n = 1$. In this case, the second term ($m = 1$) dominates in the expansion (39) for the displacement of the outer region. Figure 6 shows the resonance frequencies varying with the radius ratio b/a for a fixed thickness ratio $\frac{h_1}{h_2} = 1.1$ and outer radius $\frac{a}{h_2} = 10$. The left end of the plot corresponds to a uniform circular plate of thickness h_2, which has a cut-off frequency, $\omega_{c2} = \frac{\pi}{h_2}\sqrt{\frac{\mu}{\rho}}$, while the right end corresponds to a uniform plate of thickness h_1 with a lower cut-off frequency, $\omega_{c1} = \frac{\pi}{h_1}\sqrt{\frac{\mu}{\rho}}$ ($h_1 > h_2$). The exact solutions for the uniform circular plates are calculated from Eq. (19) with n = 1 and labeled as squares at both ends. In between, the resonance frequencies change continuously. No first-order modes can be found below the cut-off frequency ω_{c1}. Of particular interest are the vibrational modes with frequencies between the two cut-off frequencies. For these modes, the radial wave number in the outer region, $\beta_2^{(1)}$, is imaginary, and the Bessel functions describing the distributions of the displacement and the stress asymptotically reduce to those decaying exponentially from the step. Consequently, the vibration is trapped within the inner region. Figure 7 plots the mode shape associated with the point A (b/a = 0.2) in Figure 6. From (46) and (47), the approximate continuity conditions at the step (r = b) for the first-order modes are: $u_{\theta 2}^{(1)} = \Lambda_{11} u_{\theta 1}^{(1)}$ and $\sigma_{r\theta 1}^{(1)} h_1 = \Lambda_{11} \sigma_{r\theta 2}^{(1)} h_2$. Both the displacement and the stress decay exponentially from the step, which confirms the existence of trapped torsional modes in the stepped plate.

Similar analyses can be conducted for higher-order modes (e.g., n = 2, 3, …), and trapped torsional modes are expected to exist near each cut-off frequency.

C. Trapped torsional modes in infinite plates

The existence of trapped torsional modes in stepped plates offers possibilities to design an array of localized energy traps (or resonant cavities) on a large plate, each serving as a torsional-mode resonator. These resonators are very sensitive to surface loading and may be used for a variety of sensing applications. Each thickness step can be a circular mesa, for example, formed by machining, etching, or bonding of a decal onto the surface of the plate. The design parameters include the thickness and the radius of the mesa as well as the spacing between adjacent mesas. The frequencies of the trapped modes depend on the mesa dimensions, and the spacing must be large enough to avoid coupling between adjacent resonators. Each mesa thus can be considered sitting on an infinite plate ($a \to \infty$) isolated from the others. In this case, it is more convenient to use Hankel functions to describe the displacement outside the mesa, and by their asymptotic behavior only the first Hankel function remains so that the displacement at the infinite outer boundary vanishes. Therefore, any possible modes must be trapped near the mesa. Figure 8 shows the resonance frequencies for the first-order modes varying with the mesa radius for a fixed thickness ratio ($\frac{h_1}{h_2} = 1.1$). It is found that, depending on the mesa dimensions, there may exists zero, one, or multiple trapped modes. Figure 9 depicts a map for the number of trapped first-order torsional modes in a circular mesa with the radius b/h_2 and the thickness ratio h_1/h_2 as the coordinates. The map is independent of the material properties as long as the plate is homogeneous, isotropic, and elastic. The map may be read in two ways. For a circular mesa with a given thickness, there exists a critical radius, below which no trapped mode exists; multiple trapped modes may exist when the radius is large. It is often desirable to have a single trapped mode, which requires a mesa radius within the window bounded by the lowest two lines in Figure 9. Alternatively, if the mesa radius is fixed, there exists a critical thickness, below which no trapped modes can be found, and a single trapped mode exists when the thickness is within the window. Such a map may serve as a guide for designing energy-trapped torsional-mode resonators.

Comparison between the theoretical results with experiments is in progress. Preliminary results show that the predicted resonance frequencies and the mode shapes agree closely with experiments. For example, a circular mesa of radius 18.8 mm and height 0.456 mm was machined on an aluminum plate of thickness 2.642 mm, and three trapped modes were observed near the first cut-off frequency as predicted by Figure 9. The measured frequencies of the trapped modes agree with the predictions with an error less than 2%. Due to the space limit, the details of the experiments will be presented elsewhere[26].

V. Concluding Remarks

This paper presents a theoretical study of torsional vibrations in isotropic elastic plates. In particular, an approximate method is developed to analyze torsional vibrations in circular plates with thickness steps. Approximate solutions are presented for the zeroth- and first-order torsional modes. Of practical interest is the trapped first-order mode, which is theoretically predicted and confirmed by the mode shapes. The number of trapped first-order torsional modes in a circular mesa on an infinite plate are determined as functions of the normalized geometric parameters, which may serve as a guide for designing distributed torsional-mode resonators for sensing applications.

ACKNOWLEDGEMENTS

RH acknowledge College of Engineering at The University of Texas at Austin for financial support.

REFERENCES

[1] H.G. Craighead, "Nanoelectromechanical Systems", Science 290, 1532-1535 (2000).

[2] A.M. Fennimore, T.D. Yuzvinsky, W.-Q., Han, M.S., Fuhrer, J. Cumings, A. Zettl, "Rotational actuators based on carbon nanotubes", Nature 424, 408-410 (2003).

[3] P.A. Williams, S.J. Papadakis, A.M. Patel, M.R. Falvo, S. Washburn, R. Superfine, "Torsional responses and stiffening of individual multiwalled carbon nanotubes", Phys. Rev. Lett. 89, 255502 (2002).

[4] P.A. Williams, S.J. Papadakis, A.M. Patel, M.R. Falvo, S. Washburn, R. Superfine, "Fabrication of nanometer-scale mechanical devices incorporating individual multiwalled carbon nanotubes as torsional springs", Appl. Phys. Lett. 82, 805-807 (2003).

[5] D.W. Carr, S. Evoy, L. Sekaric, H.G. Craighead, J.M. Parpia, "Measurement of mechanical resonance and losses in nanometer scale silicon wires", Appl. Phys. Lett. 75, 920-922 (1999).

[6] D.J. Gorman, *Free Vibration Analysis of Beams and Shafts*, John Wiley & Sons, New York (1975).

[7] A.W. Leissa, J. So, "Comparisons of vibration frequencies for rods and beams from one-dimensional and three-dimensional analysis", J. Acoust. Soc. Am. 98, 2122-2135 (1995).

[8] J.Q. Pan, J. Pan, R.S. Ming, T. Lin, "Three-dimensional response and intensity of torsional vibrations in a stepped shaft", J. Sound and Vibration 236, 115-128 (2000).

[9] Y.Y. Kim, J.H. Kim, "Stress analysis of a stepped shaft under remote torsion", Quarterly J. Mechanics and Applied Mathematics 48, 517-530 (1995).

[10] T. Tsuiji, N. Noda, T. Shibuya, T. Koizumi, "Stress singularity in torsion problem for bonded bars", Int. J. Solids Struct. 27, 1059-1071 (1991).

[11] W. Johnson, B.A. Auld, E. Segal, F. Passarelli, "Trapped torsional modes in solid cylinders", J. Acoust. Soc. Am. 100, 285-293 (1996).

[12] R. Bechmann, Proc. IRE 49, 523 (1961).

[13] W. Shockley, D.R. Curran, D.J. Koneval, Proc. 17th Annual Freq. Control Symposium, 1963.

[14] R.D. Mindlin, P.C.Y. Lee, "Thickness-shear and flexural vibrations of partially plated, crystal plates", Int. J. Solids Struct. 2, 125-139 (1966).

[15] H.F. Tiersten, "Analysis of trapped-energy resonators operating in overtones of coupled thickness shear and thickness twist", J. Acoust. Soc. Am. 59, 879-888 (1976).

[16] P.C.Y. Lee, C. Zee, C.A. Brebbia, "Thickness shear thickness twist, and flexural vibrations of rectangular AT-cut quartz plates with patch electrodes", J. Acoust. Soc. Am. 72, 1862 (1982).

[17] H. Sekimoto, Y. Watanabe, M. Nakazawa, "Forced vibrations of thickness-flexure, face-shear and face-flexure in rectangular AT-cut quartz plates", Proc. 1992 IEEE Frequency Control Symposium, 532-536 (1992).

[18] P. C. Y. Lee, J. Wang, "Piezoelectrically forced thickness-shear and flexural vibrations of contoured quartz resonators", J. Appl. Phys. 79, 3411-3422 (1996).

[19] J. Wang, P.C.Y. Lee, D.H. Bailey, "Thickness-shear and flexural vibrations of linearly contoured crystal strips with multiprecision computation", Computers and Structures 70, 437-445 (1999).

[20] A.E.H. Love, *Mathematical Theory of Elasticity*. Cambridge University Press, New York, 1927.

[21] M. Onoe, "Contour vibrations of isotropic circular plates", J. Acoust. Soc. Am. 28, 1158-1162 (1956).

[22] A.H. Meitzler, “An ultrasonic technique for determining the elastic constants of glass wafers”, Proc. 1992 Ultrasonics Symposium, 963-968 (1992).

[23] S.K. Clark, “Torsional wave propagation in hollow cylindrical bars”, J. Acoust. Soc. Am. 28, 1163-1165 (1956).

[24] K.F. Graff, *Wave Motion In Elastic Solids*. Dover Publications, Inc., New York, 1991.

[25] J.-H. Kang, Three-dimensional vibration analysis of thick, circular and annular plates with nonlinear thickness variation. Computers and Structures 81, 1663-1675 (2003).

[26] T. Knowles, C. Bremigan, M.K. Kang, R. Huang, in preparation.

[27] D. Zhou, F.T.K. Au, Y.K. Cheung, S.H. Lo, “Three-dimensional vibration analysis of circular and annular plates via the Chebyshev-Ritz method”, Int. J. Solids Struct. 40, 3089-3105 (2003).

[28] R.D. Mindlin, “An introduction to the mathematical theory of vibrations of elastic plates”, A monograph prepared for US Army Signal Corps Engineering Laboratories, Fort Monmouth, New Jersey (1955).

[29] S.D. Poisson, “Memoire sur l’equilibre et le mouvement des corps elastiques”, Mem. Acad. Sci., Paris, Ser. 2, vol. 8, 357-570 (1829).

[30] A.L. Cauchy, “Sur l’equilibre et le mouvement d’une plaque elastique don’t l’elasticite n’est pas la meme dans tous les sens”, Exercices de Mathematique 4, 1-14 (1829).

[31] G. Kirchhoff, “Uber das Gleichqewicht und die Bewegung einer elastichen Scheibe”, Crelles J. 40, 51-88 (1850).

[32] R.D. Mindlin, “High frequency vibrations of crystal plates”, Quart. Apply. Math. 19, 51-61 (1961).

[33] H.F. Tiersten, *Linear Piezoelectric Plate Vibrations*, Plenum Press, New York, 1969.

[34] P.C.Y. Lee, S. Syngellakis, J.P. Hou, "A two-dimensional theory for high-frequency vibrations of piezoelectric crystal plates with or without electrodes", J. Appl. Phys. 61, 1249-1262 (1987).

[35] R.D. Mindlin, M. Forray, "Thickness-shear and flexural vibrations of contoured crystal plates", J. Appl. Phys. 25, 12-20 (1954).

Figure Captions:

Figure 1: Schematics of the plates: (a) a uniform circular plate; (b) an annular plate; (c) a circular plate with a thickness step.

Figure 2: Spectrum for torsional vibrations of uniform circular plates. The circles are numerical results from Zhou et al[27].

Figure 3: Radial wave number for torsional vibrations of annular plates versus the ratio between inner and outer radius.

Figure 4: Frequency spectrum of the zeroth-order torsional vibrations of circular plates with a thickness step ($h_1/h_2 = 1.1,\ a/h_2 = 10$). The open squares are the exact solutions for uniform circular plates, independent of the plate thickness.

Figure 5: Mode shapes for the zeroth-order torsional mode corresponding to point A (b/a = 0.2) in Figure 4, in a circular plate with a thickness step ($h_1/h_2 = 1.1,\ a/h_2 = 10$). The dashed line indicates the location of the thickness step.

Figure 6: Frequency spectrum of the first-order torsional vibrations of circular plates with a thickness step ($h_1/h_2 = 1.1,\ a/h_2 = 10$). The open squares are the exact solutions for uniform circular plates.

Figure 7: Mode shapes of the first-order mode corresponding to point A of Figure 6, showing the characteristic of a trapped torsional mode in a circular plate with a thickness step ($h_1/h_2 = 1.1,\ a/h_2 = 10$). The dashed line indicates the location of the step.

Figure 8: The resonant frequencies of trapped first-order torsional modes in a circular mesa on an infinite plate ($h_1/h_2 = 1.1$).

Figure 9: A map for the number of trapped first-order torsional modes in a circular mesa on an infinite plate, in the plane spanning the normalized radius and the thickness of the mesa.

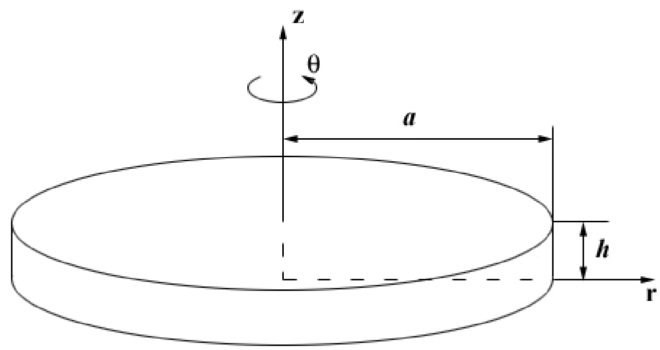

(a)

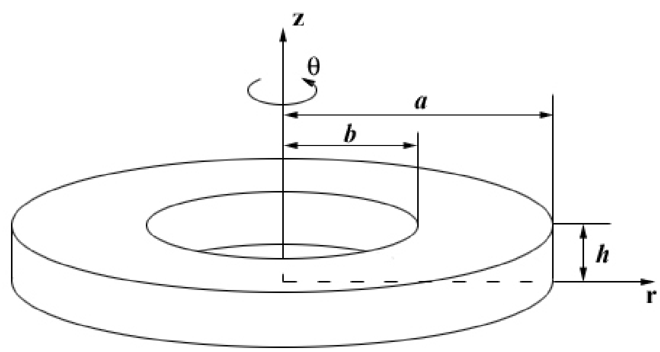

(b)

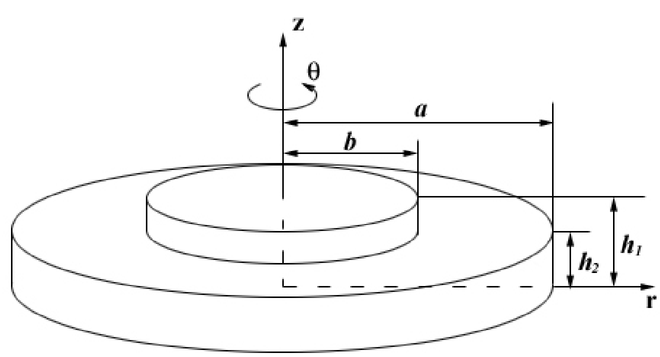

(c)

Figure 1: Schematics of the plates: (a) a uniform circular plate; (b) an annular plate; (c) a circular plate with a thickness step.

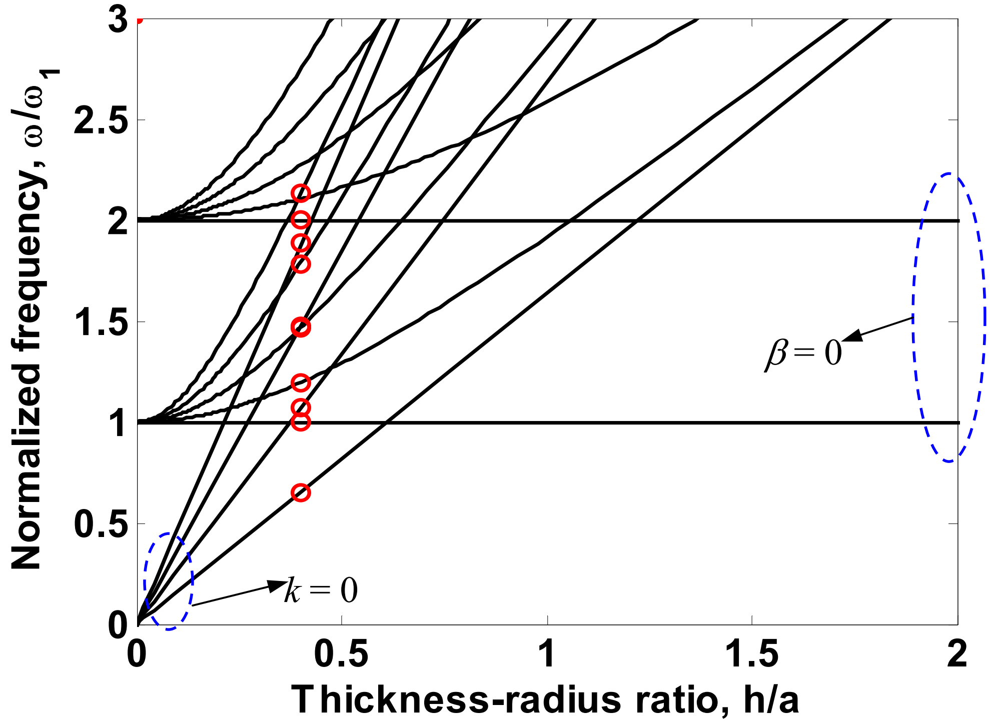

Figure 2: Spectrum for torsional vibrations of uniform circular plates. The circles are numerical results from Zhou et al[27].

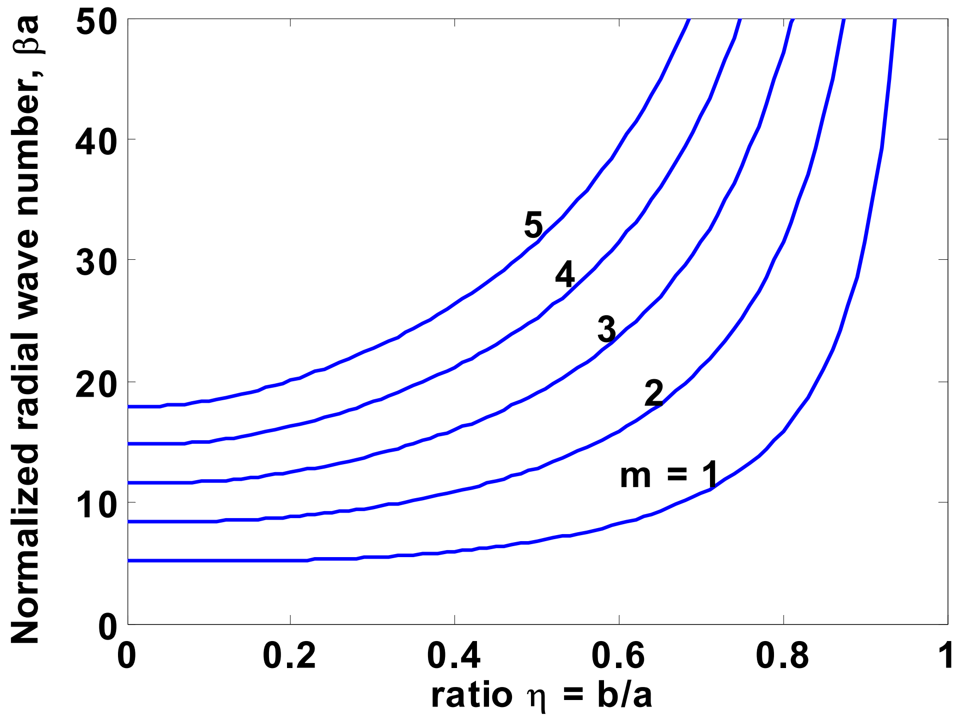

Figure 3: Radial wave number for torsional vibrations of annular plates versus the ratio between inner and outer radius.

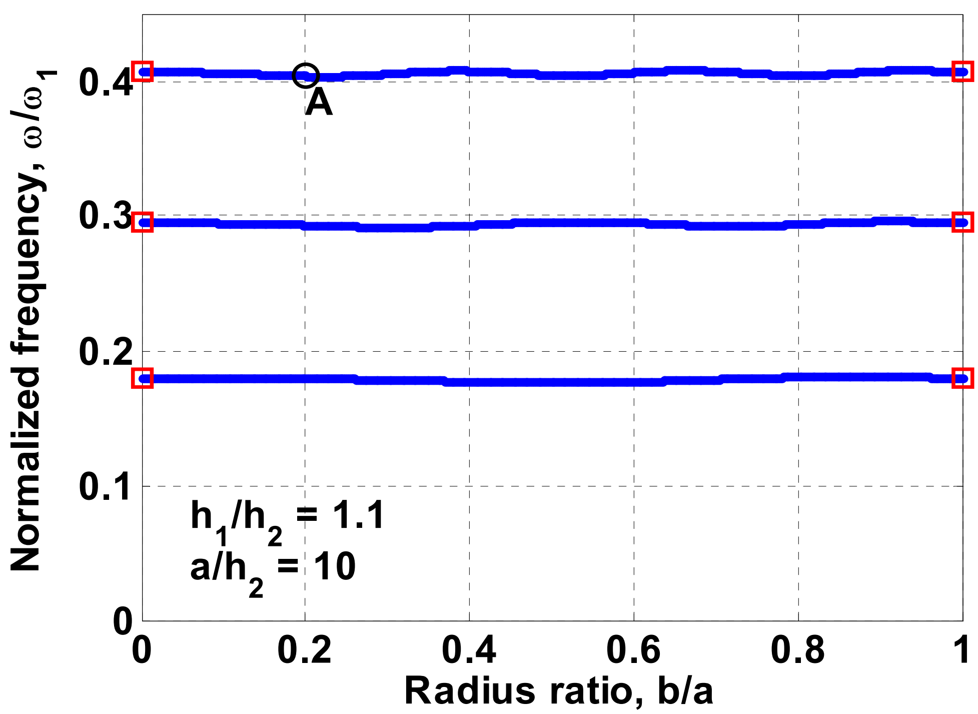

Figure 4: Frequency spectrum of the zeroth-order trosional vibrations of circular plates with a thickness step ($h_1 / h_2 = 1.1,\ a / h_2 = 10$). The open squares are the exact solutions for uniform circular plates, independent of the plate thickness.

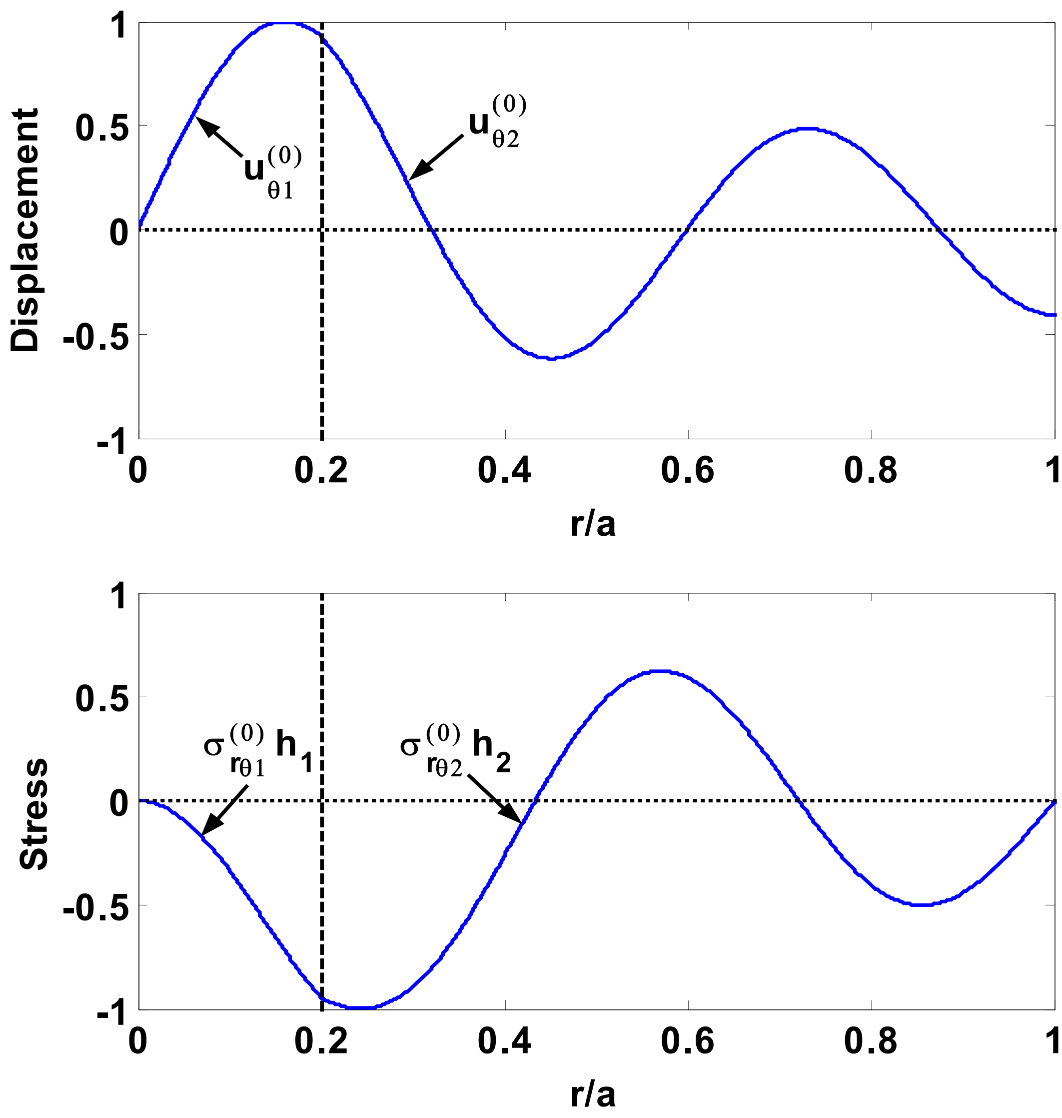

Figure 5: Mode shapes for the zeroth-order torsional mode corresponding to point A (b/a = 0.2) in Figure 4, in a circular plate with a thickness step ($h_1 / h_2 = 1.1,\ a / h_2 = 10$). The dashed line indicates the location of the thickness step.

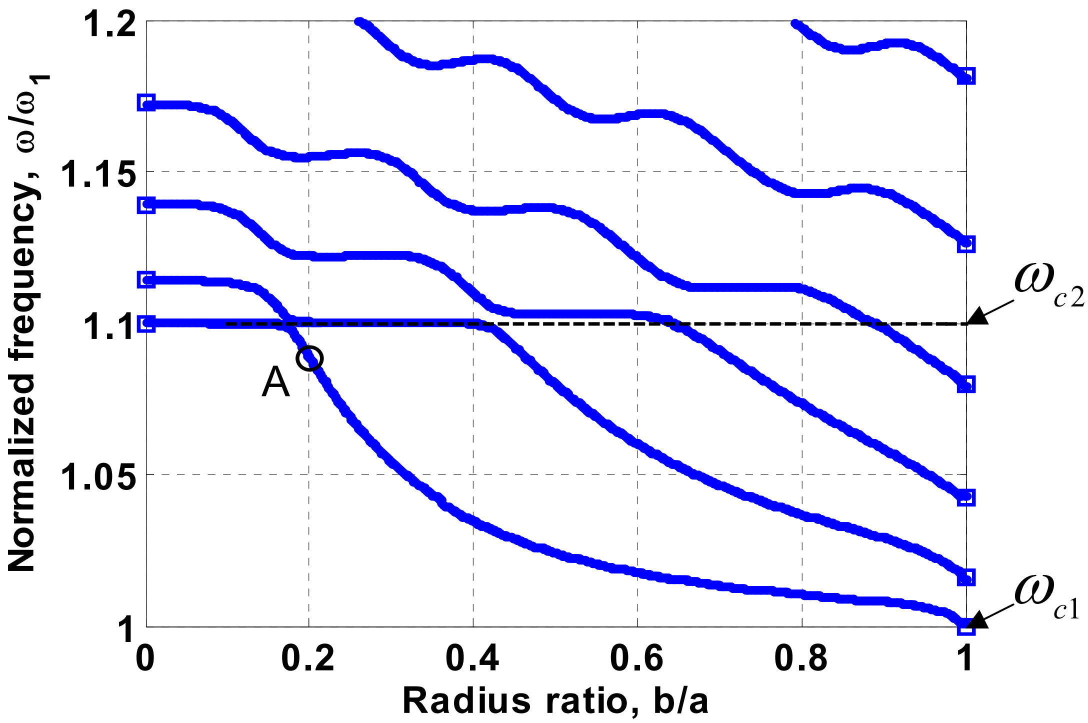

Figure 6: Frequency spectrum of the first-order torsional vibrations of circular plates with a thickness step ($h_1/h_2 = 1.1$, $a/h_2 = 10$). The open squares are the exact solutions for uniform circular plates.

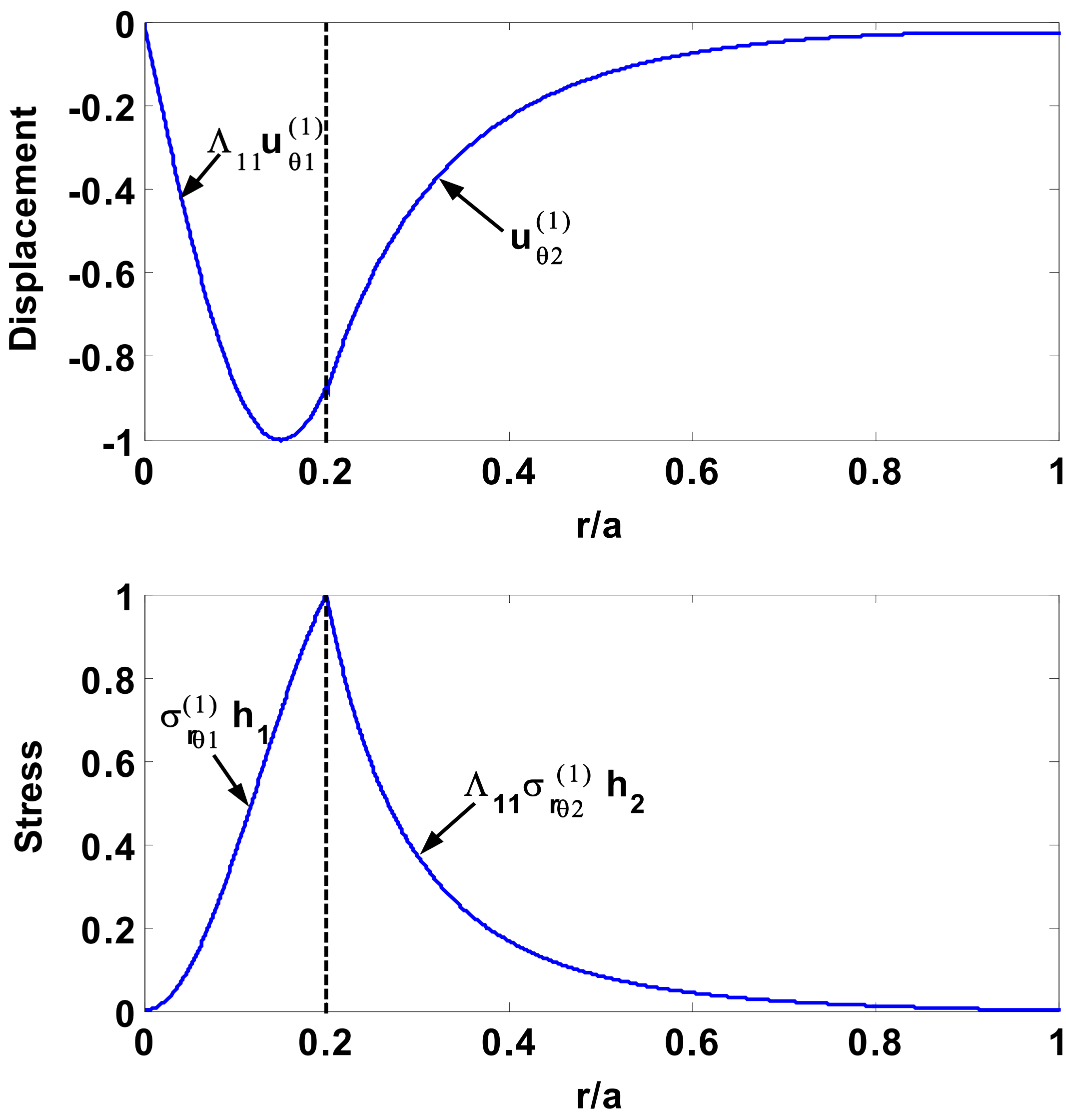

Figure 7: Mode shapes of the first-order mode corresponding to point A of Figure 6, showing the characteristic of a trapped torsional mode in a circular plate with a thickness step ($h_1/h_2 = 1.1,\ a/h_2 = 10$). The dashed line indicates the location of the step.

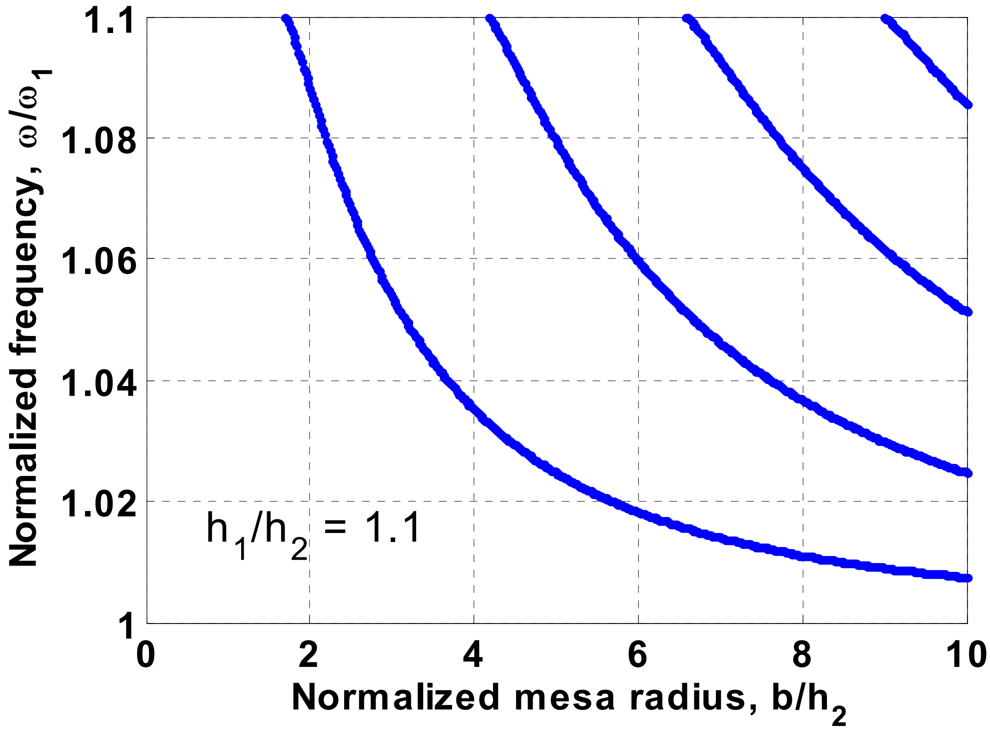

Figure 8: The resonant frequencies of trapped first-order torsional modes in a circular mesa on an infinite plate ($h_1 / h_2 = 1.1$).

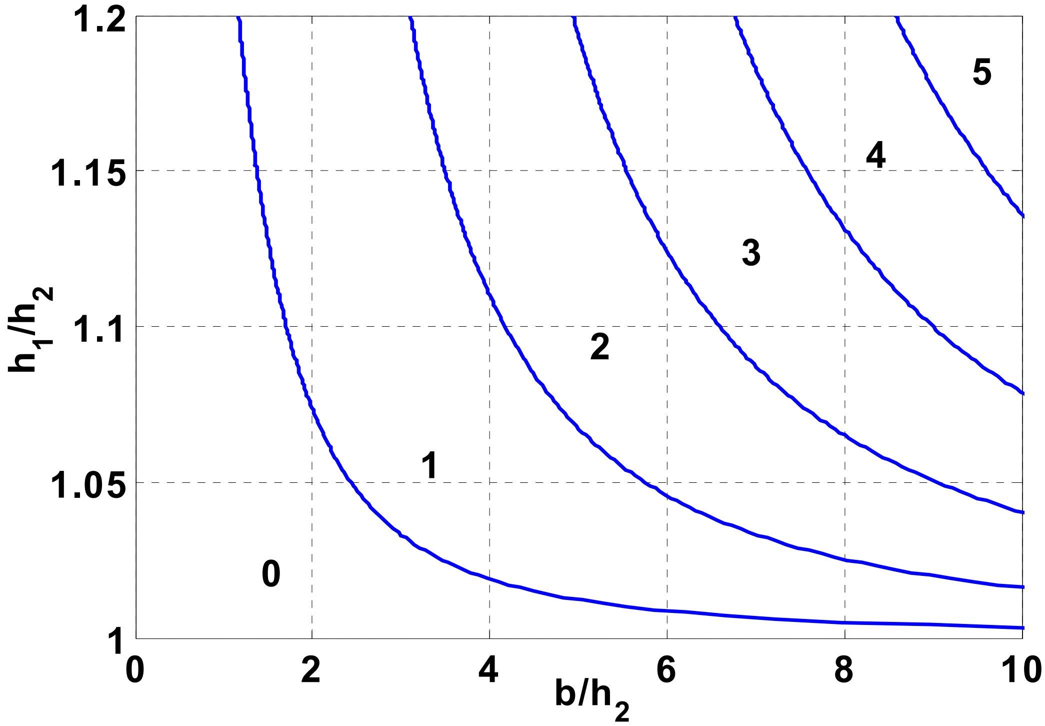

Figure 9: A map for the number of trapped first-order torsional modes in a circular mesa on an infinite plate, in the plane spanning the normalized radius and the thickness of the mesa.